TGFβ blocks STING-induced IFNα/β release and tumor rejection in spontaneous mammary tumors

Marion V. Guerin[1, 2, 3], Fabienne Regnier[1, 2, 3], Vincent Feuillet[1, 2, 3], Léne Vimeux[1, 2, 3], Julia M. Weiss[1, 2, 3,$], Thomas Guilbert[1, 2, 3], Maxime Thoreau[1, 2, 3], Gilles Renault[1, 2, 3], Veronica Finisguerra[4], Emmanuel Donnadieu [1,2, 3], Alain Trautmann[1,2, 3*] and Nadège Bercovici[1,2, 3*]

[1] Inserm, U1016, Institut Cochin, Paris, France

[2]Cnrs, UMR8104, Paris, France

[3]Université Paris Descartes, Sorbonne Paris Cité, France.

[4] Ludwig Institute for Cancer Research, Brussells, Belgium

* These authors contributed equally to this work

[$] Current address: *Division of Pediatric Hematology and Oncology, University Medical Center, Freiburg, Germany*

Key words: STING; tumor regression; type I Interferon; myeloid cells; TGFβ

Abbreviations: DMXAA: 5,6-dimethylxanthenone-4-acetic acid; IFN: interferon; IRF3: Interferon regulatory factor 3; IRF7: Interferon regulatory factor 7 ; MHCII : Major histocompatibility complex II; MMTV: Mouse mammary tumor virus; NF-κB: nuclear factor kappa-light-chain-enhancer of activated B cells; PyMT: polyomavirus middle T antigen; STING: Stimulator of interferon genes; TAM: tumor-associated macrophages; TBK1: TANK-binding kinase 1; TGFβ: tumor growth factor beta; TNFα: Tumor necrosis factor alpha.

Summary

Type I interferons (IFN) are being rediscovered as potent anti-tumoral agents. Activation of the STimulator of INterferon Genes (STING) by DMXAA can induce a strong production of IFN and the rejection of transplanted primary tumors. In the present study, we addressed whether targeting STING with DMXAA leads to the regression of spontaneous MMTV-PyMT (Spont-PyMT) mammary tumors. We show that these tumors are refractory to DMXAA-induced regression. This is due to a blockade in the phosphorylation of IRF3 and the ensuing IFNα/β production. Our study identified TGFβ, abundant in spontaneous tumors, as a key molecule limiting DMXAA-induced tumor regression: blocking TGFβ promoted infiltration of Spont-PyMT tumors by activated MHCII$^+$ tumor-associated macrophages, restored the production of IFNα following STING activation, and increased the probability of tumor regression. Based on these findings, we propose that type I IFN-dependent cancer therapies may be greatly improved by combinations including the blockade of TGFβ.

INTRODUCTION

Type I interferon (IFN) α and β are cytokines with a great potential in anti-tumor immunity. It has been shown that endogenous type I IFN may ensure a first line of defense by innate cells, promoting an adaptive immune response not only against viruses but also against cancer cells (Diamond et al., 2011; Dunn et al., 2005; Fuertes et al., 2011). In fact, modulation of immune responses by type I IFN may occur in several different ways. It often involves the regulation of cytokines and chemokines (CXCL10, CCL3, CCL2, IL-15), which are able to promote the recruitment, survival and activation of various immune cell subsets, including monocytes, dendritic cells (DC), T cells and NK cells. Moreover, IFNα induces the upregulation of MHC I and the acceleration of DC differentiation, thus improving the priming of T cells (Hervas-Stubbs et al., 2011; Santini et al., 2000). In addition, the potential of IFNα/β to inhibit protein translation can trigger conflicting signals leading to death of highly proliferating cancer or endothelial cells (Kotredes and Gamero, 2013; Sujobert and Trautmann, 2016).

Long recognized as broad immune modulators, type I IFN have been administered for years to treat cancer patients (Musella et al., 2017). However, due to the toxicity induced by its systemic administration, it is no longer commonly used as such. A new enthusiasm has followed a better understanding of the mechanisms by which type I IFN modulate immune responses. Recently, the cytosolic molecule STING has been the focus of several investigations aiming at restimulating the production of type I IFN in the tumor ecosystem. STING is ubiquitously expressed and is activated by cytosolic nucleotides derived from pathogens or self-damages. In particular, it has been shown that STING can sense endogenous cytosolic DNA promoting anti-tumor immunity (Woo et al., 2014). Synthetic cyclic dinucleotides (CDN) injected intratumorally have been shown to elicit the generation of anti-tumor specific $CD8^+$ T cells *in vivo* and the regression of transplanted tumors (Corrales et al., 2015). Endothelial cells were found to rapidly release IFNβ in the tumor of transplanted tumors treated with intratumoral CDN (Demaria et al., 2015). The DMXAA agent has the dual property of

activating STING and disrupting specifically the tumor vasculature (Baguley and Siemann, 2010). One intraperitoneal (i.p.) injection is sufficient to induce the regression of primary transplanted tumors as a single agent or in combination with vaccination ((Fridlender et al., 2013; Henare et al., 2012; Jassar et al., 2005). In line with this, we have recently reported that the DMXAA induced-regression of PyMT transplanted tumors relies on IFNα/β production and on the cooperation of T cells with myeloid cells at the tumor site (Weiss et al., 2017).

Together, these reports suggest that inducing type I IFN in solid tumors by targeting the STING pathway is a promising therapeutic approach. Nevertheless, would it be sufficient to induce the rejection of solid tumors that arise spontaneously? Multiple resistance mechanisms take place during the progression of spontaneous tumors, which is slower than that of transplanted ones. In particular, the transplantation of tumor cells induces an acute inflammation locally associated with cell death and priming of the immune cell infiltrate (Joncker et al., 2016). In contrast, spontaneous tumors emerge from a sterile microenvironment exposed to a chronic inflammation likely to condition differently the immune cell infiltrate. When spontaneous tumors emerge in an animal, the T cell repertoire shaped in the thymus and the periphery gives rise to low affinity and anergic tumor-infiltrating T cells (Wang et al., 2011). In addition, soluble factors of chronic inflammation like TGFβ are known to suppress various immune effector cells, modulate the profile of myeloid cells and promote the emergence of regulatory T cells. Thus, although transplanted tumors share some of the characteristics of immune suppressive environments, their rapid development, within days or weeks, do not integrate the various changes that occur in spontaneous tumors during months of development. In the MMTV-PyMT tumor model, Ming Li and colleagues have nicely described the progressive accumulation of suppressive tumor-associated macrophages (TAM) subsets in the mammary tumors from 8 week-to 20 week-old transgenic mice (Franklin et al., 2014). In fact, the density of such TAM, assimilated to “M2-like macrophages”, which represent a major component of the tumor microenvironment, has been correlated with a poor prognosis in various cancer types in

humans (Zhang et al., 2012). In contrast, detailed analyses of the myeloid cell compartment in human tumors revealed that the density of TAM with a M1-like phenotype correlate with a favorable prognosis in some cancers (Fridman et al., 2017). In line with this, when appropriately stimulated, macrophages can mediate anti-tumor activity, together with anti-tumor $CD8^+$ T cells, at least in transplanted tumor models (Beatty et al., 2011; Klug et al., 2013; Ma et al., 2013; Sektioglu et al., 2016; Thoreau et al., 2015; Weiss et al., 2017). Thus, the nature and the activation status of the tumor microenvironment may drastically influence the outcome of therapeutic treatments.

In the present study, we addressed whether targeting STING with DMXAA can induce the regression of spontaneous MMTV-PyMT (Spont-PyMT) mammary tumors. We show that these tumors are refractory to DMXAA-induced regression. This is related to a blockade in the phosphorylation of IRF3 and the ensuing IFNα/β production. Our study identified TGFβ, abundant in spontaneous tumors, as a key molecule limiting DMXAA-induced tumor regression: blocking TGFβ promoted infiltration of Spont-PyMT tumors by activated $MHCII^+$ TAM and restored the production of IFNα following STING activation.

RESULTS

Limited efficacy of DMXAA in the spontaneous MMTV-PYMT model

To assess if Spont-PYMT tumors developing in MMTV-PyMT mice could regress with a DMXAA treatment, as reported earlier for transplanted PyMT (Trans-PyMT) tumors (Weiss et al., 2017), we injected MMTV-PYMT mice with DMXAA when posterior tumors reached ~ 6 mm in diameter (in approximately 2 month-old mice). Five days after the DMXAA injection, very few tumors (<20%) had regressed in MMTV-PyMT mice whereas 90% of Trans-PyMT tumors did regress, as shown for comparison in Fig. 1A. The detailed follow up of individual tumors of MMTV-PyMT mice (Fig. 1B) shows that DMXAA reduced the tumor growth rate compared to control mice but tumor regression was rarely achieved.

We then examined the immune response triggered by DMXAA in Spont-PyMT tumors, compared to Trans-PyMT ones. Before treatment, the proportion of TAM ($CD11b^+$ $Ly6C^{neg}$ $Ly6G^{neg}$ $F4/80^+$), monocytes ($CD11b^+$ $Ly6C^{high}$ $Ly6G^{neg}$), neutrophils ($CD11b^+$ $Ly6G^+$) and $CD8^+$ T cells was similar between Trans-PyMT and Spont-PyMT tumors (Fig. 1C, grey bars). In both models, TAM represented the largest population of immune cells. After one injection of DMXAA, TAM, which are known to release TNFα early after DMXAA injection (Wang et al., 2009; Weiss et al., 2017), decreased rapidly and came back close to their previous level at day 4 in spontaneous tumors compared to day 8 in transplanted ones (Fig. 1C). Moreover, whereas DMXAA injection induced a strong and transient neutrophil infiltrate in Trans-PyMT at 24h (40% of the infiltrating cells), only a slight and transient infiltration (12% of the infiltrating cells) was measured in Spont-PyMT tumors. Monocytes arrived earlier in spontaneous tumors than in transplanted ones (day 1 *versus* day 4) but their numbers remained smaller. Finally, some $CD8^+$ T cells were secondarily recruited in the tumor in the following days, and reached a peak at day 8 as in the DMXAA-treated Trans-PyMT tumors. However, this

infiltrate was modest, about 4 times smaller than in Trans-PyMT tumors (8% *versus* 30% at day 8, respectively).

Altogether, these data indicate that DMXAA injection in Spont-PyMT tumors induced the recruitment of few neutrophils, monocytes and CD8 T cells, and led to a much smaller impact on tumor regression than in the transplanted tumor model.

MMTV-PyMT mice are resistant to STING-induced type I IFN production

Next, we reasoned that a difference in the tumor microenvironment could affect the cytokines and chemokines released after DMXAA injection. DMXAA activates the ubiquitous adaptor STING and subsequently triggers the production of TNFα through NFκB, the production of type I IFN through the phosphorylation of IRF3 (pIRF3) and the production of chemokines through pSTAT6 (Burdette and Vance, 2013; Roberts et al., 2007). Thus, we measured the cytokines expressed in the tumor microenvironment shortly after DMXAA injection in MMTV-PyMT mice. As shown in figure 2A, we could detect the upregulation of *Tnf*α, *Ccl2*, *Cxcl1* and *Ccl20* in Spont-PyMT tumors, like in Trans-PyMT ones (Fig. S1A), even though the fold increases could be different in the two tumor types. Strikingly, no significant increase in mRNA levels of *Ifn*α and *Ifn*β genes was detected in the spontaneous tumor model (Fig. 2A) whereas in transplanted tumors, these genes were highly expressed from 3h to 24h after DMXAA treatment (Fig. S1A). As expected, the absence of type I IFN transcripts led to an absence of IFNα production in DMXAA-treated Spont-PyMT tumors, in contrast to Trans-PyMT ones (Fig. 2B).

To test if the blunted type I IFN signaling after DMXAA injection in Spont-PyMT tumors is DMXAA-specific, we tested the TLR4 ligand LPS, another inducer of type I IFN. LPS injection induced *Ifn*α, *Ifn*β and *Tnf*α mRNA levels within 3 hours in Trans-PyMT tumors, while in Spont-PyMT tumors only

TNFα gene was upregulated by LPS (Fig. 2C). Similarly, the intra-tumoral injection of the CDN 2'3' cGAMP, another STING agonist, failed to induce the upregulation of *Ifnα* or *Ifnβ* genes in Spont-PyMT tumors (Fig. S1B). These results indicate that Spont-PyMT tumors have an intrinsic, general impairment to produce type I IFN.

Taken together, these data show that Spont-PyMT tumors have an impaired production of type I IFN in response to STING or TLR4 stimulation, which may explain the resistance to DMXAA treatment in these mice.

DMXAA fails to induce the phosphorylation of IRF3 in Spont-PyMT tumors

We next analyzed early signaling triggered downstream of STING activation. In untreated mice, there was no difference in *Sting, Irf3 and Irf7* mRNA levels between the two tumor models (Fig.S2A). The Tank binding kinase 1 (TBK1), which is responsible for the phosphorylation of IRF3, was phosphorylated in both tumor models after DMXAA treatment (Fig. S2B). This result is consistent with the upregulation of *Tnfα* and chemokines mRNA levels detected after DMXAA injection (Fig. 2A). Together, this indicates that the signaling pathway leading to type I IFN production is altered downstream of TBK1 activation.

The phosphorylation of IRF3, involved in STING- as well as LPS-signaling pathways leading to type 1 IFN production, was first measured by immunofluorescence in tumor slices from transplanted and spontaneous tumors, as soon as 3h after DMXAA injection. A strong pIRF3 labeling (unraveling cell responsiveness to STING activation by DMXAA) was detected after DMXAA treatment in slices of Trans-PyMT tumors (Fig. 3A, left panel). The pIRF3^{+} cells included tumor cells (EpCAM^{+}) and also myeloid cells (F4/80^{+}) and some endothelial (CD31^{+}) cells (Fig. 3B). By contrast, pIRF3^{+} cells were hardly detectable in tumor slices of DMXAA-treated Spont-PyMT tumors (Fig. 3A, right panel). These

results indicate that DMXAA injection failed to activate the IFN pathway in any cell type of the tumor ecosystem in MMTV-PyMT mice.

As DMXAA was first discovered as a vascular disrupting agent (Baguley and Siemann, 2010), we wondered if the vasculature of Spont-PyMT tumors was resistant to vascular damages induced by DMXAA, thus preventing indirectly the activation of the immune infiltrate. In fact, after DMXAA injection, $CD31^+$ vessels of Sont-PyMT tumors were rapidly disrupted, leading to a reduction in tumor perfusion (Fig. S3) albeit to a lesser extent than in Trans-PyMT tumors (Weiss et al., 2017). One can thus conclude that DMXAA does affect the Sont-PyMT tumor ecosystem, consistent with the production of chemokines and cytokines shown in Figure 2A. Nevertheless, the specific defect at the level of IFN production which normally contributes to the vascular damages (Roberts et al., 2008) is too weak to be really efficient in DMXAA-treated MMTV-PyMT mice.

To investigate more deeply if there was a difference in the tumor microenvironment between both tumors that could prevent the response to DMXAA, we transplanted cells freshly dissociated from Spont-PyMT tumors into a mammary gland of MMTV-PyMT mice starting to present spontaneous tumors. These mice therefore had one transplanted and several spontaneous tumors. We then checked whether IRF3 phosphorylation was prevented in all of them. About 10 days after tumor grafting, the PyMT transplanted tumor in these mice reached a diameter of ~ 6mm. In these Trans-in-Spont PyMT tumors, DMXAA was able to trigger the phosphorylation of IRF3 at a level similar to that usually measured in Trans-PyMT tumors (Fig. 3C and Fig. S2C). At the same time, the Spont-PyMT tumor next to the transplanted one showed no pIRF3 labeling whatsoever (Fig. S2C). These data indicate that the absence of DMXAA response in Spont-PyMT tumors is strictly due to its local microenvironment.

To further dissect which cell subset of the tumor microenvironment is important upon DMXAA stimulation, we first isolated tumor cells ($EpCAM^+$) from Trans-PyMT tumors, and measured the IFNα

produced in response to DMXAA stimulation *in vitro*. No IFNα was detected (Fig. S3D), suggesting that immune infiltrating cells are likely to be the main source of IFN production in response to DMXAA. Then, we compared the capacity of $CD45^+$ cells isolated from both Spont- and Trans-PyMT tumors to phosphorylate IRF3 after STING stimulation *in vitro.* We observed a profound reduction in the proportion of $pIRF3^+$ cells amongst $CD45^+$ cells in Spont-PYMT tumors (Fig. S2D). We suspected that this maybe due to different $CD45^+$ cell types which infiltrate Trans-PyMT and Spont-PyMT tumors at steady state. Even though the proportion of myeloid cells was equivalent in the two models, their phenotype was different. Indeed, compared to Trans-PyMT tumors, Spont-PyMT tumors contained much fewer activated (MHC II^+) TAM and monocytes (Fig. 3E), but twice as many $CD206^+MHCII^-$TAM (Fig. S2E).

Taken together, these results suggest that although the two models are based on the same tumor cells, the tumor microenvironment of spontaneous MMTV-PyMT mice is resistant to DMXAA-induced IFN production. This resistance seems to be related mainly to the myeloid cell fraction.

TGFβ blocks type I IFN production by immune cells

TGFβ has been shown to orientate myeloid cells towards immunosuppressive profiles and to inhibit the production of pro-inflammatory cytokines by macrophages, including IFNβ (Zhang et al., 2016). Therefore, we examined if TGFβ was involved in the impaired type I IFN production following DMXAA administration to MMTV-PyMT mice by changing the polarization of macrophages. Strikingly, TGFβ mRNA was expressed at much higher levels (~7 fold) in untreated Spont-PyMT tumors than in Trans-PyMT ones (Fig. 4A). In addition, as shown in Figure 4B, the vast majority of the cells in spontaneous tumors, and not in transplanted ones, showed nuclear pSMAD2/3 expression, indicating active signaling through TGFβR in Spont-PyMT tumors. Nuclear pSMAD 2/3 were found in all type of cells including $F4/80^+$ myeloid cells as well as in $gp38^+$ fibroblasts and $EpCAM^+$ tumor cells (Fig. 4C).

Next, we treated MMTV-PyMT mice with an anti-TGFβ antibody, and characterized the nature of immune cells in the tumors, before DMXAA treatment. We noticed that the proportion of neutrophils was increased by two fold among myeloid cells (20% *versus* <10% in anti-TGFβ *versus* control mice, respectively) at the expense of monocytes (Fig. S4A). The proportion of TAM did not change, but their phenotype did. Indeed, blockade of TGFβ restored an activated profile with a doubling of MHCII$^+$ TAM (Fig. 5A). The few infiltrating monocytes were also mainly MHC II$^+$ in anti-TGFβ treated mice.

We thus wondered if anti-TGFβ treatment rendered Spont-PyMT tumors sensitive to DMXAA. To test this, MMTV-PyMT mice were treated with an anti-TGFβ antibody for 3 days, then injected with DMXAA and sacrificed 3h later, to measure the phosphorylation of IRF3 in tumor slices. As shown in Figure 5B, the neutralization of TGFβ *in vivo* allowed the DMXAA-induced phosphorylation of IRF3. Among the pIRF3$^+$ cells, we identified both F4/80$^+$ myeloid cells and tumor cells. Moreover, this anti-TGFβ neutralization made possible the secretion of IFNα after DMXAA stimulation (Fig. 5C). To identify if TAM were the cell population responsible for IFNα production, we purified F4/80$^+$ from dissociated tumors. It then appeared that the F4/80$^+$ fraction produced a much larger amount of IFNα, compared to the negative fraction of tumor cell suspension after *in vitro* stimulation with DMXAA (Fig. 5D). Furthermore, MHC II$^+$ subsets of TAM tend to produce more IFNα than their MHC II$^-$ counterpart (Fig. S4B). Together, these results indicate that TGFβ treatment renders MMTV-PyMT mice more sensitive to DMXAA stimulation by promoting the infiltration of mammary tumors by activated MHC II$^+$ TAM capable of producing type 1 IFN.

We next wondered if the blockade of TGFβ could facilitate tumor regression induced by DMXAA in those mice. Mice were treated with a combination of anti-TGFβ during 9 days, associated with a single DMXAA injection, 3 days after the beginning of the TGFβ treatment. We observed that the majority of tumors had regressed or had stabilized at day 5 in mice receiving the combined

treatment (Fig. 5E). In addition, the non-regressing tumors grew more slowly than control or DMXAA-treated spontaneous mice.

All these results suggest that TGFβ acts on the proportion of immune cells able to produce type I IFN, and that blocking TGFβ allow DMXAA-induced IFN production and tumor regression in MMTV-PyMT mice.

Discussion

Type I IFN have the unique potential to promote the activation and recruitment of various immune effectors and represent a natural defense, mainly against viruses, which could be redirected against cancer. Encouraging results have already been obtained in transplanted tumor models with STING agonists (Corrales et al., 2015; Weiss et al., 2017). However, whether one can induce therapeutically the production of type I IFN in spontaneous tumors remained a burning question. Here, we provide an example in which TGFβ accumulation in the microenvironment of spontaneous tumors prevents the production of IFNβ/α by macrophages after STING activation and contributes to block tumor rejection. This obstacle can be overcome with an anti-TGFβ treatment.

Truncated activation of the STING/TBK1/IRF3 pathway compromises regression of Spont-*PyMT tumors*

In stark contrast with the tumor regression systematically induced by DMXAA in transplanted PyMT mice (Weiss et al., 2017), we report here that Spont-PyMT tumors rarely regress after STING activation. A weak immune response with few neutrophils, monocytes and $CD8^+$ T cells recruited at the tumor site, was associated with the resistance to DMXAA-induced tumor regression. What was specifically lacking in spontaneous tumors was the production of IFNβ and IFNα, not the production of immune-attractant chemokines. Three type I IFN inducers, DMXAA, LPS or cGAMP, all failed to induce the production of IFNβ/α in these spontaneous tumors. These results suggest that a particular feature of spontaneous tumors may interfere with the induction of anti-tumor immunity and prompted us to look for specific blunted of *ifn*β/α gene upregulation and production.

The absence of IFN mRNA was associated with a dramatic defect in IRF3 phosphorylation in the tumor ecosystem, in both tumor cells and immune infiltrating cells, after DMXAA injection in MMTV-PyMT mice. On the contrary, the activation of TBK1, necessary for the activation of IRF3, was

preserved, indicating a specific block downstream STING/TBK1 pathway. The transcription of *ifn*β, driven by pIRF3 homodimers or by pIRF3/pIRF7 heterodimers, was thus blocked at an early stage. A positive feedback loop mediated by IFNAR signaling normally allows further upregulation of *IRF7* mRNA and IFNα production. As expected, no upregulation of *irf7* gene expression took place in Spont-PyMT tumors after DMXAA compared to Trans-PyMT tumors (data not shown), probably as a direct consequence of the absence of pIRF3 and IFNβ.

Decreased responsiveness to IFNα has already been reported in cancer patients (Critchley-Thorne et al., 2009), with reduced phosphorylation of STAT1 after stimulation with IFNα *in vitro*. Our study adds a key element: next to the IFNα responsivess, the capacity to produce IFNβ and IFNα may also be compromised. Our study highlights that a defect in IFNβ/α production in a tumor may originate from an early block in STING/IRF3 signaling. This is different from the well-known defective IFNα production by tumor cells, as a result of mutations or epigenetic regulation of this pathway (Ng et al., 2018; Xia et al., 2016), which provides an advantage for therapeutic interventions with oncoviruses (Xia et al., 2016). Here, the therapeutic potential of STING agonists to boost an anti-tumor response in solid tumors relies on the capacity of the tumor microenvironment to produce type I IFN. The MMTV-PyMT mammary model illustrates that some tumors may be resistant to such interventions.

Our data further suggest that it is the tumor microenvironment that conditioned the IFNβ/α production the most, following DMXAA treatment. More specifically, endothelial cells and a large fraction of myeloid cells in Trans-PyMT tumors, strongly phosphorylated IRF3 following DMXAA injection. These results are consistent with earlier reports by Demaria and colleagues showing that endothelial cells rapidly produce IFNβ following injection of STING agonist (Demaria et al., 2015). Note however that in our experiments, endothelial cells were unlikely to be the main source of type I IFN as in Demaria's work, but represented only a minute fraction of pIRF3^{+} cells, susceptible to produce IFNβ. It should also be underlined that tumor cells were not producing IFNα *in vitro,* which reveals the existence of an additional checkpoint between pIRF3 and IFNα production. Together, our

data therefore suggest that the different abilities of Trans- and Spont-PyMT to produce type I IFN resides in different tumor microenvironment, essentially in myeloid cells.

TGFβ impairs IFNβ/a production in the tumor microenvironment of Spont-PyMT

We found that an anti-TGFβ treatment allowed DMXAA to induce the activation of IRF3, the production of IFNα, and to facilitate tumor regression. TGFβ is fundamental in many physiological functions, including the regulation of mammary gland development. Although it may inhibit cell proliferation (and therefore, initial tumor growth), frequent mutations are found in TGFβR signaling that facilitate tumor outgrowth. However, TGFβ is better known for its negative role later on, with the suppression of immune effector functions and acceleration of metastasis dissemination (Moses and Barcellos-Hoff, 2011). Not surprisingly, high levels of the active form of TGFβ have been associated with poor survival in many advanced cancer (Lin and Zhao, 2015). Of particular interest, the density of pSMAD2/3 in the stroma, downstream TGFβR signaling, has been associated with poor prognosis in non-small cell lung cancer (Chen et al., 2014). In MMTV-PyMT mice, the TGFβ mRNA level was high and nuclear pSMAD2/3 was observed in the vast majority of cells of the tumor ecosystem, indicating that the cellular source of TGFβ is unlikely to be unique. We have not attempted to identify the source of TGFβ, but it is well known that it may be secreted by multiple cell types, including macrophages (Mantovani et al., 2002) and apoptotic cells (Chen et al., 2001). Such signs of massive TGFβ signalling were never observed in Trans-PyMT tumors. The fact that an anti-TGFβ treatment of MMTV-PyMT mice restored partially their capacity to respond to DMXAA for the production of type I IFN suggested that TGFβ signaling can directly or indirectly impair the activation of STING/TBK1/IRF3 pathway. One possibility is that SMAD2 and SMAD3 directly inhibit IRF3, resulting in reduced IFNβ production (Sugiyama et al., 2012).

Another potential mode of action may be indirect. Indeed, it has been shown that TGFβR signaling is involved in the polarization of myeloid cells and the suppression of pro-inflammatory cytokines (Zhang et al., 2016). Similarly, the blockade of TGFβ signaling promote the emergence of anti-tumoral neutrophils (Fridlender et al., 2009). In our study, we found that the anti-TGFβ treatment was accompanied by an increased density of neutrophils and activated MHC II^+ TAM and monocytes that may be more prone to respond to pro-inflammatory signals. Interestingly, a human study conducted by Susuki and colleagues in human breast tumors showed that the plasmacytoid DC that accumulate in triple negative breast tumors, have a very low potency to produce type I IFN (Sisirak et al., 2012), and TGFβ was involved in this blockade (Sisirak et al., 2013).

Combination therapies with TGFβ blockade

Numerous studies have proposed explanations for the protumoral action of TGFβ. Many of them deal with the direct immunosuppressive effect of TGFβ (including their release by regulatory T cells) on T cells (Esquerré et al., 2008; Sarkar et al., 2011; Takaku et al., 2010). Others attribute it to the polarization of myeloid cells towards an immunosuppressive phenotype (Zhang et al., 2016), or to its effect on cancer-associated fibroblasts (Mariathasan et al., 2018; Tauriello et al., 2018), and thus on the ability of T cells to contact tumor cells, even though the underlying molecular mechanism of inhibition remained elusive. We propose here a new molecular mechanism by which TGFβ may exert a protumoral effect, in particular in spontaneous tumors, in which TGFβ can blunt the IFNα/β production.

Our work demonstrates that the capacity of STING agonists to exert an anti-tumoral effect should be markedly enhanced if combined with an anti-TGFβ treatment. The TGFβ/IFNβ interference highlighted here is likely to matter not only for STING agonists under active development, but also for chemotherapeutic agents like anthracyclins, for which tumor regression has been associated with

a type I IFN signature (Sistigu et al., 2014). In tumors like breast tumors that poorly respond to anti-PD1/PDL1 checkpoint inhibitors, and in which TGFβ and M2-like macrophages are abundant (Fridman et al., 2017; Moses and Barcellos-Hoff, 2011), our work shows that there would be a solid rationale for using a triple combination of anti-TGFβ, anti-PD-1 and a third partner, STING agonist or chemotherapy.

Experimental procedures

Animal studies

MMTV-PyMT transgenic mice are maintained by backcrossing on FvB/NCrl mice (Charles River laboratories). Transplanted PYMT mice were generated as described in a previous work (Weiss et al,. 2017). Briefly, fresh tumor cell suspensions were prepared from MMTV-PyMT tumor bearing mice by mechanical and enzymatic dissociation and were then injected (10^6 cells) in one mammary gland of FvB mice. Mice were maintained at the Cochin Institute SPF animal facility. Animal care was performed by expert technicians in compliance with the Federation of European Laboratory Animal Science association and under the approval of the animal experimentation ethics committee of Paris Descartes (CEEA 34, 16-063).

Mice with tumors of 6mm in diameter received a single i.p. DMXAA injection (23 mg/kg in DMSO, Sigma) or 100 µl of 50% DMSO in PBS as control. For TGFβ blockade, 200 µg of anti-TGFβ antibody (Bioxcell, clone 1D11) was injected every 2 days from days -3 to day +6 after DMXAA treatment. LPS (50 µg) or cGAMP (25 µg) were injected i.p. or i.t. respectively and mice were sacrificed 3 hours later. Tumor cell suspensions for *in vitro* experiments or flow cytometry characterization were prepared by mechanical and enzymatic dissociation (Weiss et al., 2017).

Multicolor flow cytometry

Tumor cells suspension ($4x10^6$) were stained in 96-wells round bottom plates with live/dead staining (Blue fluorescent reactive dye, Invitrogen) during 20 minutes at room temperature. Fc receptors were blocked with anti-FcR (anti-CD16 CD-32 at 5µg/ml, BD Pharmingen). After 2 washes in PBS 2% FCS, cells were stained with the following antibodies CD45-AF700, CD11b-BV421, Ly6C-APCCy7, Ly6G-BV510, F4.80 BV650, IA/IE-BV785, CD206-PE, CD64-APC, CD11c-PeCy7 (for myeloid and MHC II

staining), with CD45-AF700, TCRβ-BV605, CD4-BV711 and CD8-PerCPef710 antibodies (for lymphoid staining) antibodies, all purchased from BD Pharmingen. After washing in PBS, cells were fixed in 1% PFA, stored at 4°C, and acquired the next day with LSR II flow cytometer (BD Bioscience). For detection of phosphorylated proteins staining, cell suspensions were stimulated 3h with DMXAA 250µg/ml, fixed immediately in PFA 4%, permeabilized with frozen methanol 90%, stained overnight with pIRF3-AF647 or pTBK1-PE (from Ozyme), washed and analyzed by multicolor flow cytometry.

Immunofluorescence

Tumor pieces were fixed overnight with Periodate-Lysine-Paraformaldehyde at 4°C. Immunofluorescence on thick tumor slices (350 µm) was performed as previously described (Bougherara et al., 2015). Immunostaining of surface markers was performed at 37°C for 15 min with antibodies specific for EpCAM-BV421, F4/80-AF488 or AF647, Gp38-PEor CD31-PE (all from BD Pharmingen). For additional intracellular staining, tissue slices were fixed in 4% PFA (10min RT) and permeabilized with methanol 90% 30min at 4°C. For detection of pSMAD2/3, primary anti-pSMAD2/3 Ab was revealed with anti-rabbit Alexa 488 (cell signaling).

Images were obtained using a confocal spinning-disk (CSU-X1; Yokogawa) upright microscope (DM6000FS; Leica) equipped with a ORCA Flash4.0LT camera (Hamamatsu) and a 25x 0.95NA W objective (Leica). All images were acquired with MetaMorph 7 imaging software (Molecular Devices) and analyzed with Image J homemade routines.

Transcriptomic analysis

Tumor RNA was extracted using a RNeasy Mini Kit (Qiagen) according to the manufacturer's instructions. The RNA were reverse transcribed using the Advantage® RT for PCR kit (Applied

Clontech) and gene expression was analyzed by RT-qPCR with the LighCycler® 480 Real-Time PCR system. The list of primers that were used are provided in the supplementary table 1.

ELISA

The IFNα production test was performed on entire tumor cell suspensions obtained after Ficoll density separation (Histopaque-1093 from Sigma) or after cell sorting and then stimulated overnight with 250 µg/ml of DMXAA. The ELISA test was performed using IFNα Mouse ELISA Kit (Thermo Fisher) according to the manufacturer's instructions.

Statistics

Unless otherwise indicated, results are expressed as means ± SEM of 3 to 8 mice and result from 2 to 4 independent experiments. . Data were analyzed with GraphPad Prism5 software. p values were calculated by the unpaired Student's t test or One-way ANOVA and Tukey test for multiple comparison. Values ≤ 0.05 were considered significant. * $p<0.05$; ** $p<0.01$; *** $p<0.001$).

Supplemental information: Supplemental Information includes 5 figures.

Author contributions:

M.G. and N.B. designed the experiments, M.G., F.R., V.F., L.V., J.M.W., V.F., N.B. and M.T. performed and analysed the experiments. G.R. and F.R. performed the contrast-enhanced ultrasound measurements, T.G. helped for image analysis with Image J. N.B. and A.T. designed the study and M.G., A.T and N.B. wrote the manuscript and prepared the figures.

Acknowledgements:

We are really grateful to G. Bismuth and C. Katari Mimoun for their critical review of the manuscript and their helpful suggestions, and the staff of the IMAG'IC, CYBIO and GENOM'IC facilities of the Cochin Institute for their advice all along this study.

Funding support:

This work was granted by Worldwide Cancer Research, the "Comité de Paris de La Ligue Contre le Cancer", the Cancer Research for Personalized Medicine (CARPEM), CNRS, INSERM and University Paris-Descartes. M. G. was granted by the Ministère de l'Education Nationale, de l'Enseignement Supérieur et de la Recherche.

Conflict of interests statement : The authors have declared that no conflict of interest exists

References

Baguley, B.C., and Siemann, D.W. (2010). Temporal Aspects of the Action of ASA404 (Vadimezan; DMXAA). Expert Opin. Investig. Drugs *19*, 1413–1425.

Beatty, G.L., Chiorean, E.G., Fishman, M.P., Saboury, B., Teitelbaum, U.R., Sun, W., Huhn, R.D., Song, W., Li, D., Sharp, L.L., et al. (2011). CD40 Agonists Alter Tumor Stroma and Show Efficacy Against Pancreatic Carcinoma in Mice and Humans. Science *331*, 1612–1616.

Bougherara, H., Mansuet-Lupo, A., Alifano, M., Ngô, C., Damotte, D., Le Frère-Belda, M.-A., Donnadieu, E., and Peranzoni, E. (2015). Real-Time Imaging of Resident T Cells in Human Lung and Ovarian Carcinomas Reveals How Different Tumor Microenvironments Control T Lymphocyte Migration. Front. Immunol. *6*, 500.

Burdette, D.L., and Vance, R.E. (2013). STING and the innate immune response to nucleic acids in the cytosol. Nat. Immunol. *14*, 19–26.

Chen, W., Frank, M.E., Jin, W., and Wahl, S.M. (2001). TGF-beta released by apoptotic T cells contributes to an immunosuppressive milieu. Immunity *14*, 715–725.

Chen, Y., Xing, P., Chen, Y., Zou, L., Zhang, Y., Li, F., and Lu, X. (2014). High p-Smad2 expression in stromal fibroblasts predicts poor survival in patients with clinical stage I to IIIA non-small cell lung cancer. World J. Surg. Oncol. *12*.

Corrales, L., Glickman, L.H., McWhirter, S.M., Kanne, D.B., Sivick, K.E., Katibah, G.E., Woo, S.-R., Lemmens, E., Banda, T., Leong, J.J., et al. (2015). Direct Activation of STING in the Tumor Microenvironment Leads to Potent and Systemic Tumor Regression and Immunity. Cell Rep. *11*, 1018–1030.

Critchley-Thorne, R.J., Simons, D.L., Yan, N., Miyahira, A.K., Dirbas, F.M., Johnson, D.L., Swetter, S.M., Carlson, R.W., Fisher, G.A., Koong, A., et al. (2009). Impaired interferon signaling is a common immune defect in human cancer. Proc. Natl. Acad. Sci. U. S. A. *106*, 9010–9015.

Demaria, O., De Gassart, A., Coso, S., Gestermann, N., Di Domizio, J., Flatz, L., Gaide, O., Michielin, O., Hwu, P., Petrova, T.V., et al. (2015). STING activation of tumor endothelial cells initiates spontaneous and therapeutic antitumor immunity. Proc. Natl. Acad. Sci. U. S. A. *112*, 15408–15413.

Diamond, M.S., Kinder, M., Matsushita, H., Mashayekhi, M., Dunn, G.P., Archambault, J.M., Lee, H., Arthur, C.D., White, J.M., Kalinke, U., et al. (2011). Type I interferon is selectively required by dendritic cells for immune rejection of tumors. J. Exp. Med. *208*, 1989–2003.

Dunn, G.P., Bruce, A.T., Sheehan, K.C.F., Shankaran, V., Uppaluri, R., Bui, J.D., Diamond, M.S., Koebel, C.M., Arthur, C., White, J.M., et al. (2005). A critical function for type I interferons in cancer immunoediting. Nat. Immunol. *6*, 722–729.

Esquerré, M., Tauzin, B., Guiraud, M., Müller, S., Saoudi, A., and Valitutti, S. (2008). Human regulatory T cells inhibit polarization of T helper cells toward antigen-presenting cells via a TGF-beta-dependent mechanism. Proc. Natl. Acad. Sci. U. S. A. *105*, 2550–2555.

Franklin, R.A., Liao, W., Sarkar, A., Kim, M.V., Bivona, M.R., Liu, K., Pamer, E.G., and Li, M.O. (2014). The cellular and molecular origin of tumor-associated macrophages. Science *344*, 921–925.

Fridlender, Z.G., Sun, J., Kim, S., Kapoor, V., Cheng, G., Ling, L., Worthen, G.S., and Albelda, S.M. (2009). Polarization of tumor-associated neutrophil phenotype by TGF-beta: “N1” versus “N2” TAN. Cancer Cell *16*, 183–194.

Fridlender, Z.G., Jassar, A., Mishalian, I., Wang, L.-C., Kapoor, V., Cheng, G., Sun, J., Singhal, S., Levy, L., and Albelda, S.M. (2013). Using macrophage activation to augment immunotherapy of established tumours. Br. J. Cancer *108*, 1288–1297.

Fridman, W.H., Zitvogel, L., Sautès-Fridman, C., and Kroemer, G. (2017). The immune contexture in cancer prognosis and treatment. Nat. Rev. Clin. Oncol. *14*, 717–734.

Fuertes, M.B., Kacha, A.K., Kline, J., Woo, S.-R., Kranz, D.M., Murphy, K.M., and Gajewski, T.F. (2011). Host type I IFN signals are required for antitumor CD8+ T cell responses through CD8α+ dendritic cells. J. Exp. Med. *208*, 2005–2016.

Henare, K., Wang, L., Wang, L.-C.S., Thomsen, L., Tijono, S., Chen, C.-J.J., Winkler, S., Dunbar, P.R., Print, C., and Ching, L.-M. (2012). Dissection of stromal and cancer cell-derived signals in melanoma xenografts before and after treatment with DMXAA. Br. J. Cancer *106*, 1134–1147.

Hervas-Stubbs, S., Perez-Gracia, J.L., Rouzaut, A., Sanmamed, M.F., Bon, A.L., and Melero, I. (2011). Direct Effects of Type I Interferons on Cells of the Immune System. Clin. Cancer Res. *17*, 2619–2627.

Jassar, A.S., Suzuki, E., Kapoor, V., Sun, J., Silverberg, M.B., Cheung, L., Burdick, M.D., Strieter, R.M., Ching, L.-M., Kaiser, L.R., et al. (2005). Activation of tumor-associated macrophages by the vascular disrupting agent 5,6-dimethylxanthenone-4-acetic acid induces an effective CD8+ T-cell-mediated antitumor immune response in murine models of lung cancer and mesothelioma. Cancer Res. *65*, 11752–11761.

Joncker, N.T., Bettini, S., Boulet, D., Guiraud, M., and Guerder, S. (2016). The site of tumor development determines immunogenicity via temporal mobilization of antigen-laden dendritic cells in draining lymph nodes. Eur. J. Immunol. *46*, 609–618.

Klug, F., Prakash, H., Huber, P.E., Seibel, T., Bender, N., Halama, N., Pfirschke, C., Voss, R.H., Timke, C., Umansky, L., et al. (2013). Low-dose irradiation programs macrophage differentiation to an $iNOS^{+}$/M1 phenotype that orchestrates effective T cell immunotherapy. Cancer Cell *24*, 589–602.

Kotredes, K.P., and Gamero, A.M. (2013). Interferons as inducers of apoptosis in malignant cells. J. Interferon Cytokine Res. Off. J. Int. Soc. Interferon Cytokine Res. *33*, 162–170.

Lin, R.-L., and Zhao, L.-J. (2015). Mechanistic basis and clinical relevance of the role of transforming growth factor-β in cancer. Cancer Biol. Med. *12*, 385–393.

Ma, Y., Adjemian, S., Mattarollo, S.R., Yamazaki, T., Aymeric, L., Yang, H., Portela Catani, J.P., Hannani, D., Duret, H., Steegh, K., et al. (2013). Anticancer Chemotherapy-Induced Intratumoral Recruitment and Differentiation of Antigen-Presenting Cells. Immunity *38*, 729–741.

Mariathasan, S., Turley, S.J., Nickles, D., Castiglioni, A., Yuen, K., Wang, Y., Kadel, E.E., Koeppen, H., Astarita, J.L., Cubas, R., et al. (2018). TGFβ attenuates tumour response to PD-L1 blockade by contributing to exclusion of T cells. Nature *554*, 544–548.

Moses, H., and Barcellos-Hoff, M.H. (2011). TGF-β Biology in Mammary Development and Breast Cancer. Cold Spring Harb. Perspect. Biol. *3*.

Musella, M., Manic, G., De Maria, R., Vitale, I., and Sistigu, A. (2017). Type-I-interferons in infection and cancer: Unanticipated dynamics with therapeutic implications. Oncoimmunology *6*.

Ng, K.W., Marshall, E.A., Bell, J.C., and Lam, W.L. (2018). cGAS-STING and Cancer: Dichotomous Roles in Tumor Immunity and Development. Trends Immunol. *39*, 44–54.

Roberts, Z.J., Goutagny, N., Perera, P.-Y., Kato, H., Kumar, H., Kawai, T., Akira, S., Savan, R., van Echo, D., Fitzgerald, K.A., et al. (2007). The chemotherapeutic agent DMXAA potently and specifically activates the TBK1-IRF-3 signaling axis. J. Exp. Med. *204*, 1559–1569.

Roberts, Z.J., Ching, L.-M., and Vogel, S.N. (2008). IFN-beta-dependent inhibition of tumor growth by the vascular disrupting agent 5,6-dimethylxanthenone-4-acetic acid (DMXAA). J. Interferon Cytokine Res. Off. J. Int. Soc. Interferon Cytokine Res. *28*, 133–139.

Santini, S.M., Lapenta, C., Logozzi, M., Parlato, S., Spada, M., Di Pucchio, T., and Belardelli, F. (2000). Type I Interferon as a Powerful Adjuvant for Monocyte-Derived Dendritic Cell Development and Activity in Vitro and in Hu-Pbl-Scid Mice. J. Exp. Med. *191*, 1777–1788.

Sarkar, A., Donkor, M.K., and Li, M.O. (2011). T cell- but not tumor cell-produced TGF-β1 promotes the development of spontaneous mammary cancer. Oncotarget *2*, 1339–1351.

Sektioglu, I.M., Carretero, R., Bender, N., Bogdan, C., Garbi, N., Umansky, V., Umansky, L., Urban, K., von Knebel-Döberitz, M., Somasundaram, V., et al. (2016). Macrophage-derived nitric oxide initiates T-cell diapedesis and tumor rejection. Oncoimmunology *5*, e1204506.

Sisirak, V., Faget, J., Gobert, M., Goutagny, N., Vey, N., Treilleux, I., Renaudineau, S., Poyet, G., Labidi-Galy, S.I., Goddard-Leon, S., et al. (2012). Impaired IFN-α Production by Plasmacytoid Dendritic Cells Favors Regulatory T-cell Expansion That May Contribute to Breast Cancer Progression. Cancer Res. *72*, 5188–5197.

Sisirak, V., Vey, N., Goutagny, N., Renaudineau, S., Malfroy, M., Thys, S., Treilleux, I., Labidi-Galy, S.I., Bachelot, T., Dezutter-Dambuyant, C., et al. (2013). Breast cancer-derived transforming growth factor-β and tumor necrosis factor-α compromise interferon-α production by tumor-associated plasmacytoid dendritic cells. Int. J. Cancer *133*, 771–778.

Sistigu, A., Yamazaki, T., Vacchelli, E., Chaba, K., Enot, D.P., Adam, J., Vitale, I., Goubar, A., Baracco, E.E., Remédios, C., et al. (2014). Cancer cell-autonomous contribution of type I interferon signaling to the efficacy of chemotherapy. Nat. Med. *20*, 1301–1309.

Sugiyama, Y., Kakoi, K., Kimura, A., Takada, I., Kashiwagi, I., Wakabayashi, Y., Morita, R., Nomura, M., and Yoshimura, A. (2012). Smad2 and Smad3 are redundantly essential for the suppression of iNOS synthesis in macrophages by regulating IRF3 and STAT1 pathways. Int. Immunol. *24*, 253–265.

Sujobert, P., and Trautmann, A. (2016). Conflicting Signals for Cancer Treatment. Cancer Res. *76*, 6768–6773.

Takaku, S., Terabe, M., Ambrosino, E., Peng, J., Lonning, S., McPherson, J.M., and Berzofsky, J.A. (2010). Blockade of TGF-β enhances tumor vaccine efficacy mediated by CD8+ T cells. Int. J. Cancer J. Int. Cancer *126*, 1666.

Tauriello, D.V.F., Palomo-Ponce, S., Stork, D., Berenguer-Llergo, A., Badia-Ramentol, J., Iglesias, M., Sevillano, M., Ibiza, S., Cañellas, A., Hernando-Momblona, X., et al. (2018). TGFβ drives immune evasion in genetically reconstituted colon cancer metastasis. Nature *554*, 538–543.

Thoreau, M., Penny, H.L., Tan, K., Regnier, F., Weiss, J.M., Lee, B., Johannes, L., Dransart, E., Le Bon, A., Abastado, J.-P., et al. (2015). Vaccine-induced tumor regression requires a dynamic cooperation between T cells and myeloid cells at the tumor site. Oncotarget *6*, 27832–27846.

Wang, L.-C.S., Thomsen, L., Sutherland, R., Reddy, C.B., Tijono, S.M., Chen, C.-J.J., Angel, C.E., Dunbar, P.R., and Ching, L.-M. (2009). Neutrophil influx and chemokine production during the early phases of the antitumor response to the vascular disrupting agent DMXAA (ASA404). Neoplasia N. Y. N *11*, 793–803.

Wang, S.-F., Fouquet, S., Chapon, M., Salmon, H., Regnier, F., Labroquère, K., Badoual, C., Damotte, D., Validire, P., Maubec, E., et al. (2011). Early T Cell Signalling Is Reversibly Altered in PD-1+ T Lymphocytes Infiltrating Human Tumors. PLoS ONE *6*, e17621.

Weiss, J.M., Guérin, M.V., Regnier, F., Renault, G., Galy-Fauroux, I., Vimeux, L., Feuillet, V., Peranzoni, E., Thoreau, M., Trautmann, A., et al. (2017). The STING agonist DMXAA triggers a cooperation between T lymphocytes and myeloid cells that leads to tumor regression. Oncoimmunology *6*, e1346765.

Woo, S.-R., Fuertes, M.B., Corrales, L., Spranger, S., Furdyna, M.J., Leung, M.Y.K., Duggan, R., Wang, Y., Barber, G.N., Fitzgerald, K.A., et al. (2014). STING-Dependent Cytosolic DNA Sensing Mediates Innate Immune Recognition of Immunogenic Tumors. Immunity *41*, 830–842.

Xia, T., Konno, H., and Barber, G.N. (2016). Recurrent Loss of STING Signaling in Melanoma Correlates with Susceptibility to Viral Oncolysis. Cancer Res. *76*, 6747–6759.

Zhang, F., Wang, H., Wang, X., Jiang, G., Liu, H., Zhang, G., Wang, H., Fang, R., Bu, X., Cai, S., et al. (2016). TGF-β induces M2-like macrophage polarization via SNAIL-mediated suppression of a pro-inflammatory phenotype. Oncotarget *7*, 52294–52306.

Zhang, Q., Liu, L., Gong, C., Shi, H., Zeng, Y., Wang, X., Zhao, Y., and Wei, Y. (2012). Prognostic Significance of Tumor-Associated Macrophages in Solid Tumor: A Meta-Analysis of the Literature. PLoS ONE *7*.

FIGURE LEGENDS

Figure 1. DMXAA induced a weak immune infiltrate but no systematic regression of Spont-PyMT tumors. (A) The proportion of tumors that regress, stabilize or progress are shown for Spont-PyMT and Trans-PyMT. **(B)** Size changes of individual tumor in MMTV-PyMT mice following injection of DMXAA (top) or DMSO as control (Bottom). The average curves are shown in color. **(C)** The proportion of TAM, neutrophils, monocytes and $CD8^+$ T cells infiltrating Spont-PyMT and Trans-PyMT tumors were determined by flow cytometry before treatment (grey bars) and at days 1 to 8 after DMXAA injection (black bars). In this and subsequent figures, the statistical significance is given by * $p<0.05$, ** $p<0.01$, *** $p<0.001$.

Figure 2. Lack of type I IFN triggering in Spont-PyMT tumors. (A) mRNA levels of *Tnfα* and chemokines, but not *Ifn*β and *Ifn*α, were upregulated in the tumors of MMTV-PyMT mice after DMXAA injection. **(B)** *In vitro,* DMXAA induced a much higher production of IFNα in Trans-PyMT compared to Spont-PyMT tumor cell suspensions. IFNα released in the supernatant was measured by ELISA after overnight stimulation with DMXAA (250 μg/ml). **(C)** One injection of LPS in MMTV-PyMT mice failed to induce the upregulation of *Ifn*β and *Ifn*α mRNA levels despite the upregulation of *Tnfα.* LPS injection in Trans-PyMT tumors induced the upregulation of *Ifn*β, *Ifn*α and *Tnfα* genes.

Figure 3. Absence of IRF3 phosphorylation in tumor cells and immune infiltrates in Spont-PyMT tumors after DMXAA treatment. (A) Trans-PyMT (left) and Spont-PyMT (right) tumors 3 hours after DMXAA treatment. Staining of tumor slices revealed numerous areas with $pIRF3^+$ cells around and within $EpCAM^+$ tumor islets in Trans- but not in Spont-PyMT tumors. **(B) In** Trans-PyMT tumors, $pIRF3^+$ cells also included myeloid cells ($F4/80^+$) and endothelial ($CD31^+$) cells. **(C)** A cell suspension of freshly dissociated Spont-PyMT tumors was transplanted into the mammary gland of a recipient

MMTV-PyMT mouse as described in *Material and Methods*. After 11 days, mice received one injection of DMXAA and 3 hours later, the transplanted tumors (Trans→ Spont) were collected and tumor slices stained for pIRF3. The fraction of pIRF3$^+$ area was quantified. Trans→ Spont tumors showed pIRF3 levels similar to thoses of Trans-PyMT tumors. Data from 2 to 4 mice/condition. **(D)** Sorted EpCAM$^+$ cells do not produce detectable IFNα after DMXAA stimulation *in vitro*. **(E)** The proportion of MHC II$^+$ TAM and monocytes were larger in untreated Trans-PyMT tumors than in Spont-PyMT tumors as determined by flow cytometry on fresh tumor cell suspensions.

Figure 4. The accumulation of TGFβ in Spont-PyMT but not in Trans-PyMT tumors impaired the activation of IRF3 and the production of IFN after DMXAA activation. (A) mRNA level of TGFβ in Trans- and Spont-PyMT tumors before treatment. **(B)** Detection of pSMAD2/3$^+$ staining in tumor slices reflecting an active TGFβR signaling in Spont-PyMT (right) but not in Trans-PyMT (left) tumors. **(C)** pSMAD2/3$^+$ cells included some myeloid cells (F4/80$^+$), fibroblasts (gp38$^+$) but the largest fraction were tumor cells (EpCAM$^+$). Arrows point to examples of the 3 cell types that are particularly clear.

Figure 5. Blocking TGFβ allows DMXAA-induced type I IFN production and the regression of Spont-PyMT tumors. (A) The proportions of intratumoral activated (MHC II$^+$) TAM and monocytes were increased in MMTV-PyMT mice treated with anti-TGFβ. **(B)** pIRF3 could be detected in myeloid cells and tumor cells after DMXAA injection in anti-TGFβ treated MMTV-PyMT mice. **(C)** IFNα production in response to DMXAA was partially restored in anti-TGFβ-treated MMTV-PyMT mice. **(D)** IFNα is mainly produced by myeloid cells: F4/80$^+$ cells from tumor cell suspension of anti-TGFβ treated MMTV-PyMT mice were isolated (F4/80$^+$) prior to DMXAA stimulation. Their IFNα production was compared to that of the F4/80$^-$ depleted fraction. **(E)** The anti-TGFβ treatment allowed a transient regression and tumor growth control after DMXAA in Spont-PyMT mice. Fold changes in tumor size at day 5 are shown for MMTV-PyMT mice treated with DMSO (CTRL), DMXAA alone or anti-TGFβ (day -5, day-3, day-1 and day3) in combination with DMXAA (day0). Each bar corresponds to an individual

tumor. The number of tumors showing regression, stabilization or progression are indicated on top. Data are derived from 3-5 mice from 3 independent experiments.

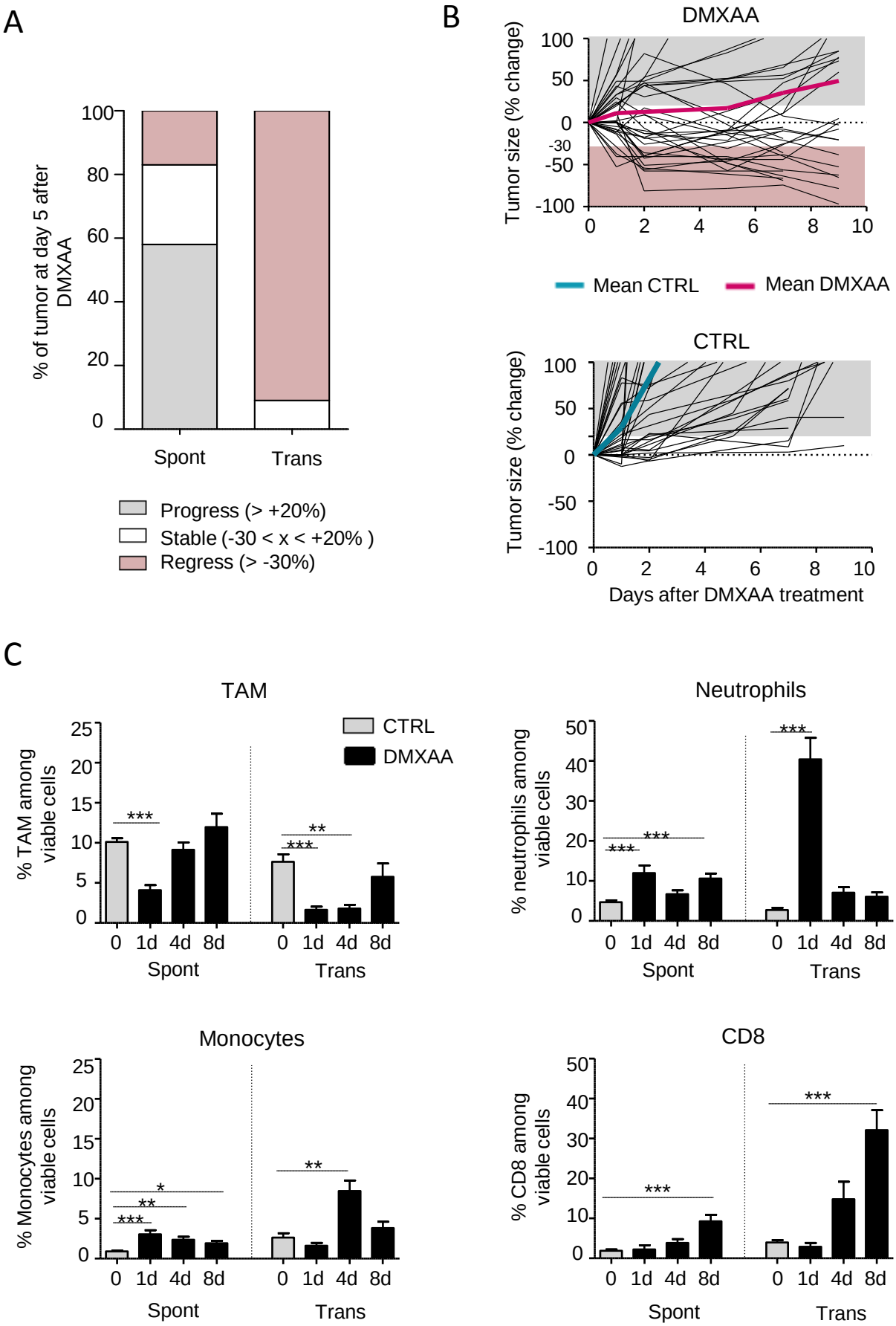
A
% of tumor at day 5 after DMXAA
100
80
60
40
20
0
Spont
Trans
Progress (> +20%)
Stable (-30 < x < +20%)
Regress (> -30%)
B
DMXAA
Tumor size (% change)
100
50
0
-30
-50
-100
0
2
4
6
8
10
Mean CTRL
Mean DMXAA
CTRL
Tumor size (% change)
Days after DMXAA treatment
C
TAM
CTRL
DMXAA
% TAM among viable cells
0
1d
4d
8d
Spont
Trans
Neutrophils
% neutrophils among viable cells
Monocytes
% Monocytes among viable cells
CD8
% CD8 among viable cells

Fig 1

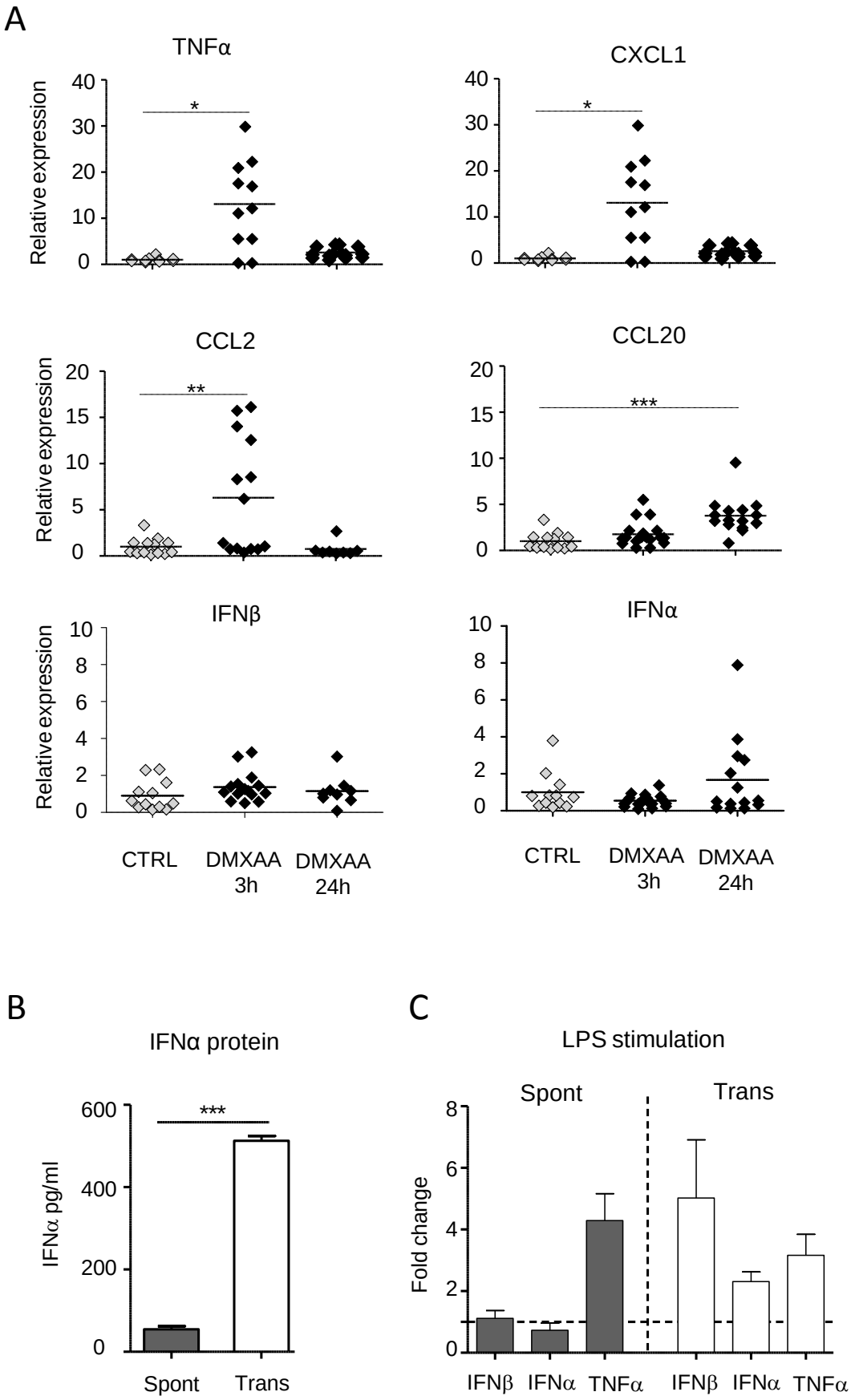
A
TNFα
CXCL1
CCL2
CCL20
IFNβ
IFNα
Relative expression
CTRL
DMXAA 3h
DMXAA 24h
B
IFNα protein
IFNα pg/ml
Spont
Trans
C
LPS stimulation
Spont
Trans
Fold change
IFNβ
IFNα
TNFα

Fig 2

A

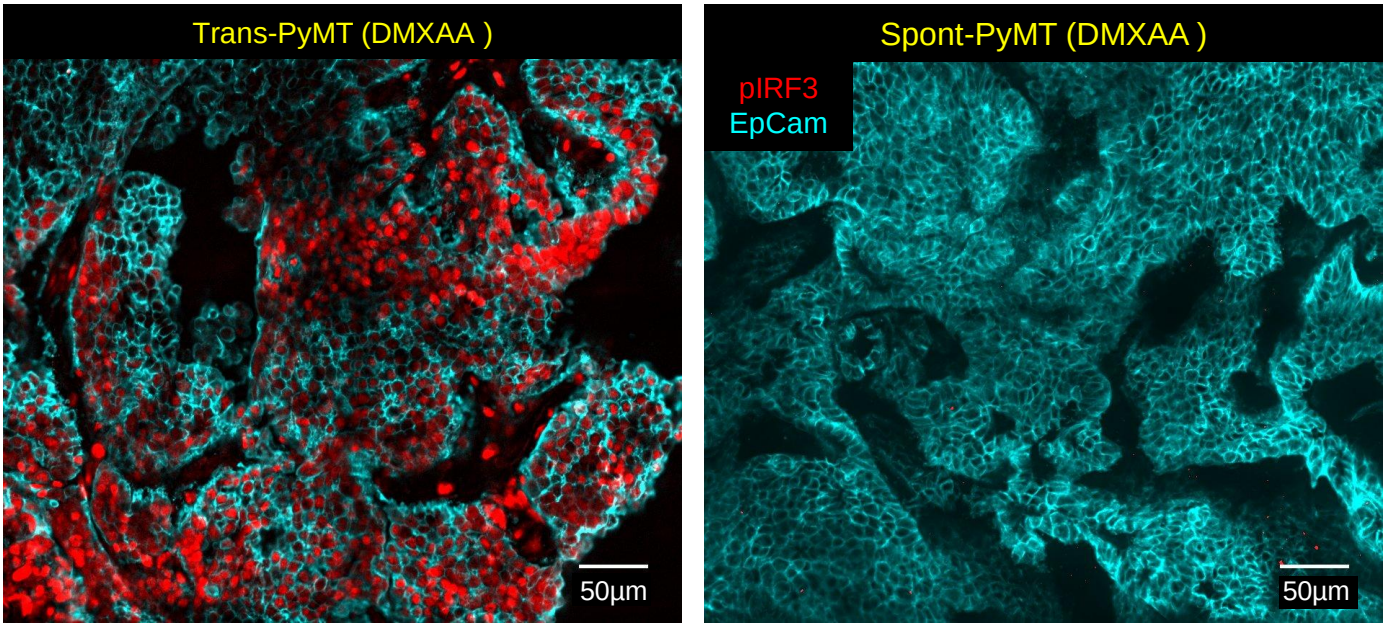
Trans-PyMT (DMXAA)
50µm
Spont-PyMT (DMXAA)
pIRF3
EpCam
50µm

B

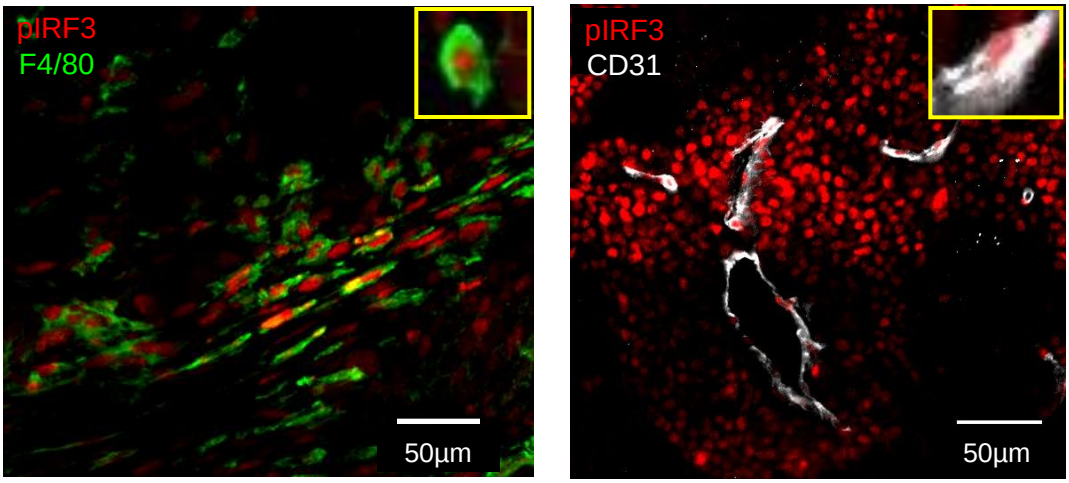
pIRF3
F4/80
50µm
pIRF3
CD31
50µm

C

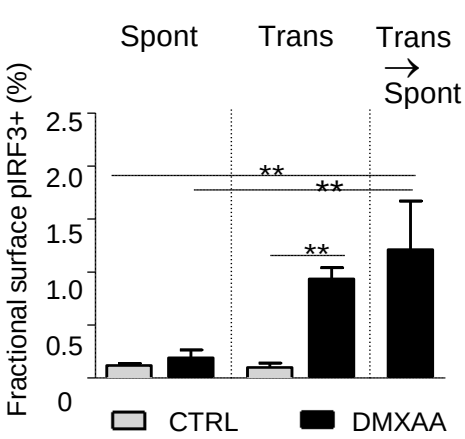
Spont
Trans
Trans → Spont
Fractional surface pIRF3+ (%)
2.5
2.0
1.5
1.0
0.5
0
**
**
**
CTRL
DMXAA

D

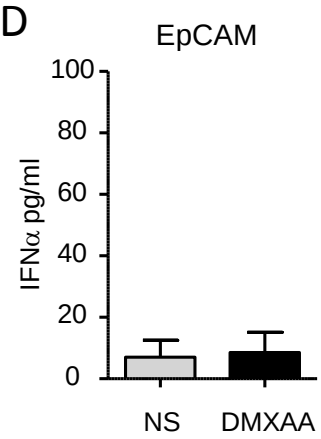
EpCAM
IFNα pg/ml
100
80
60
40
20
0
NS
DMXAA

E

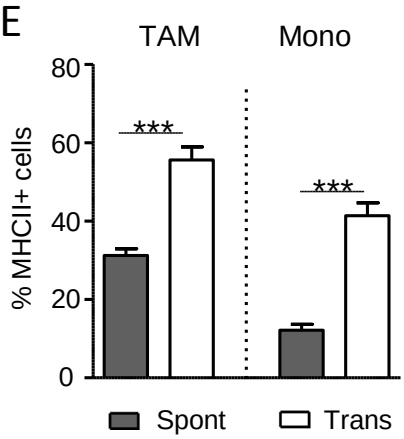
TAM
Mono
% MHCII+ cells
80
60
40
20
0
***
***
Spont
Trans

Fig 3

A

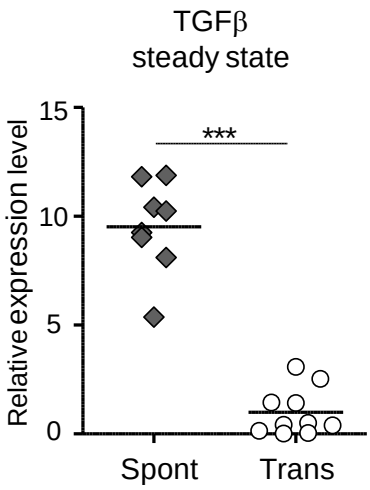
TGFβ
steady state
Relative expression level
15
10
5
0
***
Spont
Trans

B

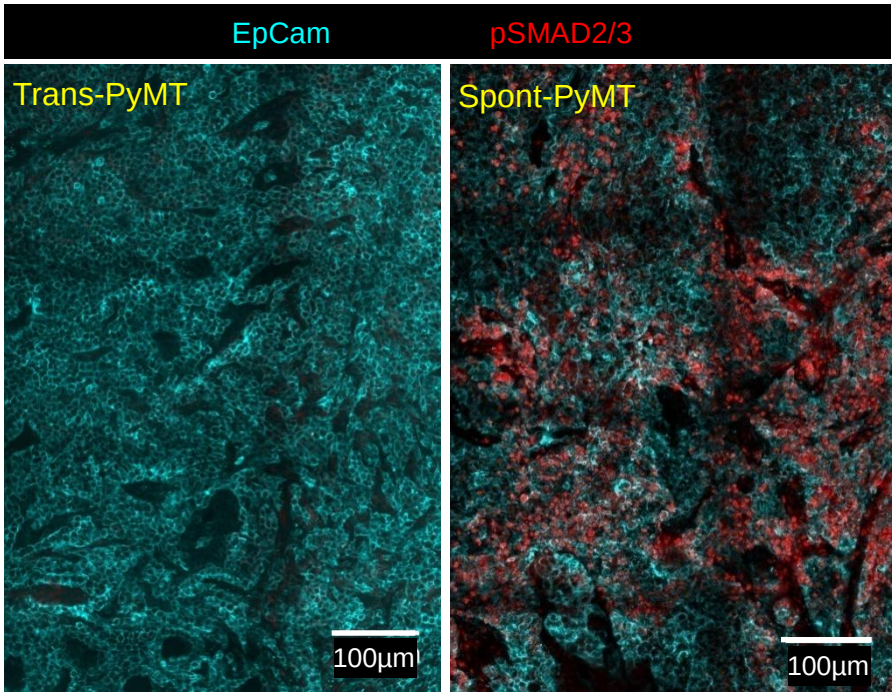
EpCam
pSMAD2/3
Trans-PyMT
Spont-PyMT
100µm
100µm

C

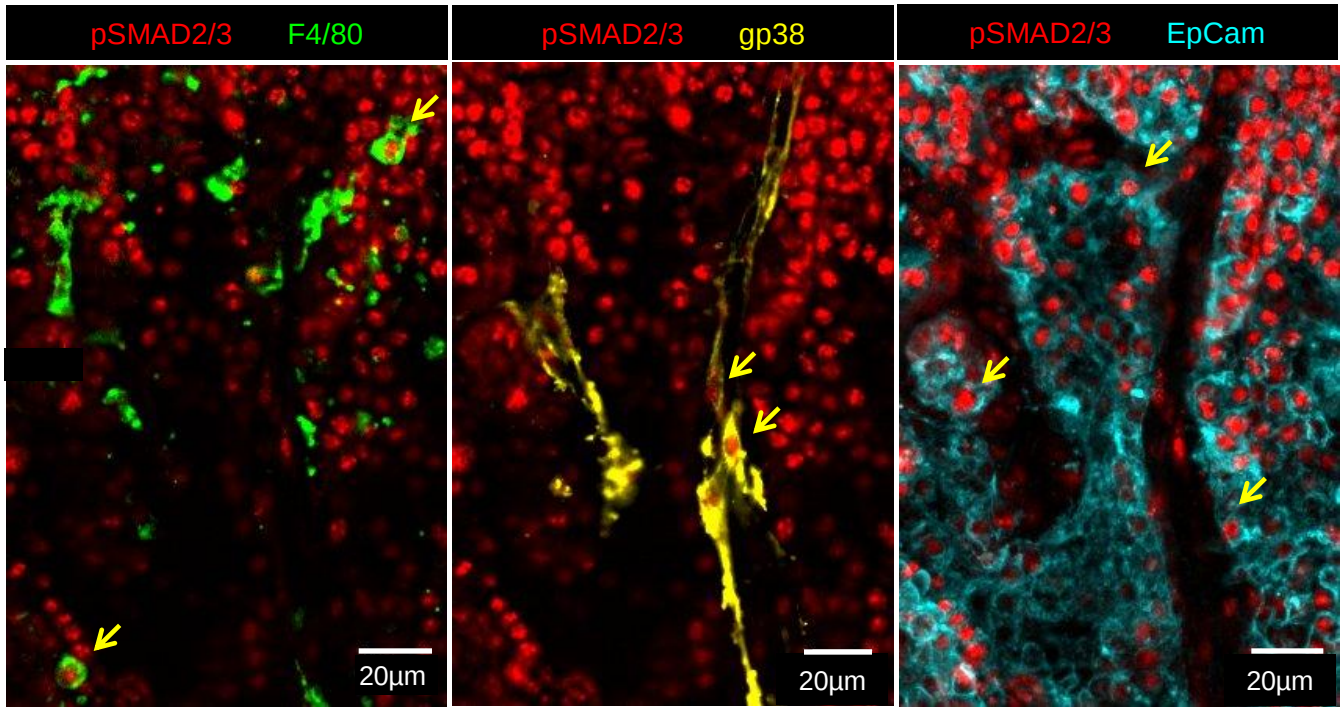
pSMAD2/3
F4/80
pSMAD2/3
gp38
pSMAD2/3
EpCam
20µm
20µm
20µm

Fig 4

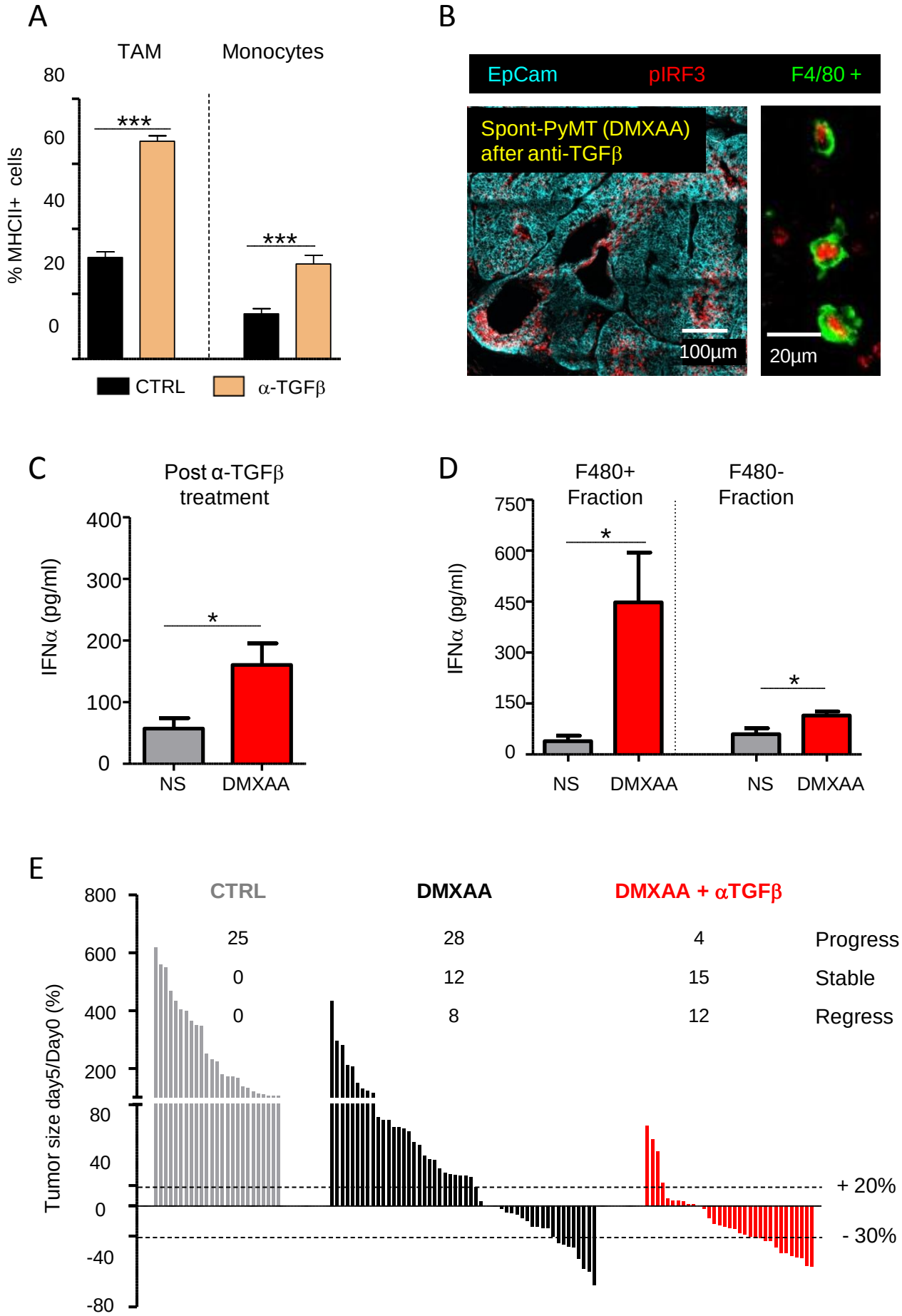
A
TAM
Monocytes
% MHCII+ cells
80
60
40
20
0
***
***
CTRL
α-TGFβ
B
EpCam
pIRF3
F4/80 +
Spont-PyMT (DMXAA)
after anti-TGFβ
100µm
20µm
C
Post α-TGFβ
treatment
IFNα (pg/ml)
400
300
200
100
0
*
NS
DMXAA
D
F480+
Fraction
F480-
Fraction
IFNα (pg/ml)
750
600
450
300
150
0
*
*
NS
DMXAA
NS
DMXAA
E
CTRL
DMXAA
DMXAA + αTGFβ
25
28
4
Progress
0
12
15
Stable
0
8
12
Regress
Tumor size day5/Day0 (%)
800
600
400
200
80
40
0
-40
-80
+ 20%
- 30%

Fig 5